

# Experimental and computational studies of Si-doped fullerenes

I.M.L. Billas, F. Tast, W. Branz, N. Malinowski, M. Heinebrodt, T.P. Martin, M. Boero<sup>a</sup>, C. Massobrio<sup>b</sup>, and M. Parrinello

Max-Planck Institut für Festkörperphysik, Heisenbergstrasse 1, D-70569 Stuttgart, Germany

Received: 1 September 1998 / Received in final form: 10 December 1998

**Abstract.** Silicon in-cage doped fullerenes result from laser-induced photofragmentation of mixed clusters of composition  $C_{60}Si_x$ . These parent clusters are produced in a low pressure condensation cell, through the mixing of silicon vapor with a vapor containing the preformed  $C_{60}$  molecules. The geometric and the electronic structures of fullerenes substitutionally doped with one and two silicon atoms are studied by *ab-initio* calculations within density functional theory.

**PACS.** 36.40.-c Atomic and molecular clusters – 61.48.+c Fullerene and fullerene-related materials – 71.24.+q Electronic structure of clusters and nanoparticles

## 1 Introduction

Doping and functionalization of fullerene molecules have aroused a growing interest both from the experimental and from the theoretical point of view. The large effort devoted to the study of doped fullerenes is motivated by the fact that doping induces important modifications in the electronic properties of the pure fullerenes. This enhances their chemical reactivity without altering the closed three dimensional structure of the cage. Beside endohedral and exohedral doping of fullerenes, substitutional doping represents a very interesting possibility for functionalizing the fullerene molecule. The first indication that such exotic molecules exist came from the mass spectra of fullerenes substitutionally doped with up to six boron atoms [1]. Soon after this discovery, experimental evidence was provided for in-cage doping with one N atom [2]. On the theoretical side, *ab initio* calculations suggested that in-cage doping of fullerenes with B and N leads to an electronic behavior similar to deep impurities in semiconductors with acceptor ( $C_{59}B$ ) and donor ( $C_{59}N$ ) states [3, 4]. Experimentally, the challenge is to produce these exotic species in macroscopic quantity and to isolate them. The doped fullerenes can then be used as building blocks for new heterogeneous nanoscale materials. This has been achieved in the case of nitrogen doped fullerenes which could be isolated in form of dimers  $(C_{59}N)_2$  [5]. In this case, a metallic intercalation compound  $K_6C_{59}N$ , isostructural to the insulating  $K_6C_{60}$  has been synthesized and investigated [6].

Recently, several groups have demonstrated the existence of other substitutionally doped fullerenes, in particu-

lar with silicon [7–10], as well as with transition metals (TM) such as Nb [11], and Fe, Co, Ni, Rh and Ir [12]. Silicon-doping of the fullerene cage with one and two Si atoms has been evidenced in mass-spectroscopic studies [7, 9, 10] and in ion mobility measurements [8]. The existence of fullerenes doped with more than two Si atoms cannot be evidenced by the direct analysis of the mass spectra due to a mass coincidence, within the experimental mass resolution, between the mass of three Si atoms and that of seven C atoms. However photofragmentation studies have unambiguously shown the existence of fullerenes doped with at least three Si atoms [10]. In these experiments, Si-doped fullerenes have been produced by laser-vaporization of a pellet of graphite and Si powders. In our experiments, an alternative method for the fabrication of in-cage Si doped fullerenes is employed. The precursor material consists of clusters composed of a fullerene molecule decorated by a various number of Si atoms. The transformation from exohedrally to substitutionally doped fullerenes is achieved through irradiation by means of laser light as explained in the next section. Little is known about the details of the substitution mechanism of C atoms of the fullerene network by heteroatoms. Experimental studies of TM in-cage doped fullerenes indicate that at least two heteroatoms must reside on the cage in order for the substitution process to occur. While one of the heteroatom M binds to a C atom and leaves the cage in the form of a MC molecule, the other fills the hole left by the missing C atom [12].

From the chemist point of view, Si doped fullerenes give rise to very interesting questions concerning the nature of the silicon-carbon bonding. In fact, though C and Si belong to the same group in the Periodic Table, their chemistry is rather different. While carbon can form single, double and triple bonds, Si has a tendency for four-fold coordination. However the Si atom incorporated in the fullerene network sits in an environment which has a  $sp^2$ - character. With re-

<sup>a</sup> Present address: JRCAT-ATP, 1-1-4 Higashi, Ibaraki 305, Tsukuba-shi, Japan

<sup>b</sup> Permanent address: IPCMS-GEMME, 23 rue de Loess, F-67037 Strasbourg, France

spect to these issues, the *ab-initio* calculations presented in Sects. 3 and 4 will give some insight into how the Si atom is bound to its nearest neighbors in the fullerene network and what kind of cage deformation it induces. Both the single and the double in-cage substitution are considered in our calculations.

## 2 Experimental

In our mass-spectrometric investigations, clusters of the composition  $C_{60}Si_x$  are generated in an inert gas condensation cell filled with about 1 mbar of He and cooled down at liquid nitrogen temperature [13, 14]. Silicon vapor is produced by laser vaporization of a Si target located in the condensation cell. This vapor mixes with the  $C_{60}$  vapor produced from a resistively heated oven and is quenched by the cold He atmosphere. It is possible to monitor the experimental parameters, like the oven temperature, the power of the vaporization laser and the helium pressure, such that the mixed clusters produced contain almost exclusively one  $C_{60}$  molecule and a various number of Si atoms. The clusters are then transported from the condensation cell through a nozzle and a differential pumping stage into a high vacuum chamber where they are photoionized by a pulsed ArF excimer laser and mass analysed in a time-of-flight mass spectrometer.

At low excimer laser fluences, we observe a distribution of clusters of composition  $C_{60}Si_x$ . The number of Si atoms contained in the  $C_{60}Si_x$  clusters covers a rather small range, up to a few Si atoms. This can be contrasted with investigations of exohedrally doped fullerenes with alkalis or alkaline earth metals, as well as with transition metals, where a much larger number of metal atoms can be brought onto the fullerene surface [14, 15]. Photofragmentation of the  $C_{60}Si_x$  clusters is achieved by increasing the excimer laser intensity. In this case, the clusters are simultaneously ionized and heated up at a temperature such that evaporation and fragmentation take place. The resulting photoionization mass spectrum is depicted in Fig. 1.

In this mass spectrum two series of peaks can be observed corresponding to clusters having an even total number of atoms and a composition  $C_{59-2n}Si$  and  $C_{58-2n}Si_2$  ( $n = 0, \dots, 10$ ). These two series exhibit the typical abundance pattern reminiscent of the fullerene geometry, where clusters with a total number of atoms of 44 and 50 are more abundant than other peaks in the series. Due to mass coincidence, peaks at the masses corresponding to fullerenes doped with more than two Si atoms cannot be uniquely assigned to these clusters. In Fig. 1, mass peaks belonging to the clusters  $C_{57}Si_3$  and  $C_{64}$ , as well as to  $C_{56}Si_4$  and  $C_{63}Si$  coincide within experimental resolution.

## 3 Computational details

Our first-principles investigations of silicon in-cage doped fullerenes  $C_{59}Si$  and  $C_{58}Si_2$  have been performed within

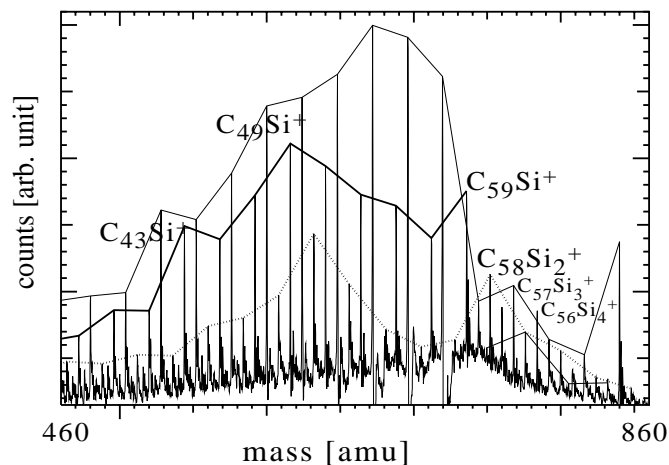


**Fig. 1.** Photoionization mass spectrum of  $C_{60}Si_x$  clusters exposed to high laser fluence. Due to intense heating, successive evaporation of carbon dimers from  $C_{60}$  results in the series of peaks corresponding to small fullerenes  $C_{60-2m}$  ( $m \geq 1$ ). The presence of  $C_{70}$  in the mass spectrum is due to trace quantity of  $C_{70}$  in the  $C_{60}$  powder material used. More importantly, clusters with composition  $C_{59-2n}Si$  and  $C_{58-2n}Si_2$  ( $n = 0, \dots, 10$ ) are observed in the mass spectrum. Notice that peaks labeled in italics at the masses of  $C_{57}Si_3$  and  $C_{56}Si_4$  are mass coincident with peaks corresponding to  $C_{64}$  and  $C_{63}Si$ , respectively.

the framework of the *ab-initio* molecular dynamics introduced by Car and Parrinello [16]. We adopted norm-conserving pseudopotentials of the Trouiller-Martins type [17]. The unit cell of our face-centred cubic periodic array has an edge of 21.16 Å, much larger than the diameter of the optimized structures of the doped fullerenes. The energy cutoff in the expansion of the Kohn-Sham (KS) orbitals in plane waves is 40 Rydberg. The structures of the doped fullerenes are optimized self-consistently starting with the structure of  $C_{60}$  and substituting one and two C atoms by Si atoms.

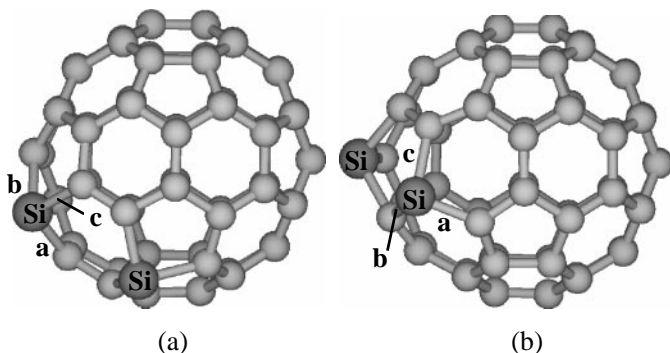
## 4 Results of the calculations

### 4.1 Geometric structures of $C_{59}Si$ and $C_{58}Si_2$

We will first consider  $C_{59}Si$  for which the fully relaxed geometric structure has been calculated. The silicon atom induces a deformation on the fullerene network which is confined to the local environment of the dopant atom. In particular, the two single and the double Si–C bonds are about 24% longer than the corresponding single and double bonds of  $C_{60}$  as shown in Table 1. Here the terminology for single and double Si–C bonds is used in a purely geometrical sense. A “single bond” is a bond between one hexagon and one pentagon and a “double bond” is a bond between two hexagons. Notice that in molecules, typical silicon-carbon bond lengths are 1.88 Å for chemical single Si–C and 1.70 Å for chemical double Si=C bonds. The structures of the  $C_{59}Si$  cation and anion are very similar

**Table 1.** Structural characteristics of  $C_{59}Si$ , its cation and its anion and comparison with C–C distances in  $C_{60}$ . Both the minimal and the maximal values of the C–C bond lengths are indicated.

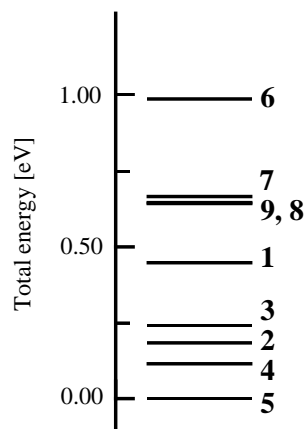
	$C_{59}Si$	$C_{59}Si^+$	$C_{59}Si^-$	$C_{60}^{\text{theory}}$	$C_{60}^{\text{exp}}$ [18]
Si–C (double bond) (Å)	1.848	1.856	1.887	—	—
Si–C (single bond) (Å)	1.901	1.888	1.926	—	—
C–C (double bond) (Å)	1.404–1.432	1.403–1.439	1.405–1.439	1.406–1.407 <sup>a</sup>	1.401(10)
C–C (single bond) (Å)	1.463–1.504	1.450–1.522	1.457–1.512	1.460–1.461 <sup>a</sup>	1.458(6)

<sup>a</sup> this work.**Fig. 2.** Ball and stick representation of two isomers of  $C_{58}Si_2$ : (a) isomer **5** which is the lowest energy configuration and (b) isomer **4**. The Si–C bond lengths for each Si atom are in (a)  $a = 1.862$  Å,  $b = 1.883$  Å,  $c = 1.922$  Å and in (b)  $a = 1.822$  Å,  $b = 1.892$  Å,  $c = 1.930$  Å.

to that of their neutral counterpart. As shown in Table 1, the variations of the Si–C bond lengths of the charged species with respect to those of neutral  $C_{59}Si$  are limited to less than 1% in the cation and to 1%–2% in the anion. As the result of the Si in-cage doping, most of the C–C single and double bond lengths of  $C_{59}Si$  are slightly increased compared to the corresponding values in the  $C_{60}$  cage (up to 3%–4%, see Table 1) and their distribution is not as sharply peaked as in  $C_{60}$ .

A self-consistent structure optimization of the doped fullerene  $C_{58}Si_2$  has been performed for a total of nine isomers, comprising all configurations where the two Si atoms are 1st (isomers **1** and **2**), 2nd (isomers **3** and **4**) and 3rd (isomers **5**, **6** and **7**) nearest neighbors (n.n.). The last two configurations considered correspond to one of 4th n.n. isomers (isomer **8**) and one where the two Si atoms lie on opposite sides of the cage (isomer **9**). Isomers **4** and **5** are depicted in Fig. 2. In all the structures considered, the conjugation pattern reflected in the bond length pattern is preserved and the Si–C bond lengths considered range from 1.82 Å and 1.93 Å.

Energetically, the relaxed structures of the various isomers considered lie within about 1 eV with energy differences between next lying configurations of 0.1 eV up to 0.35 eV as can be observed in Fig. 3. The lowest energy configuration among the nine isomers is isomer **5** depicted in Fig. 2a. It lies 0.11 eV lower in energy than the isomer **4** shown in Fig. 2b. Recent calculations which have considered the isomers **2**, **4** and **9** are in good agreement with our results [10]. Notice that in the lowest energy configuration,

**Fig. 3.** Energetics of the nine  $C_{58}Si_2$  isomers considered in our study. **1**: 1st n.n. Si at an edge between two hexagons, **2**: 1st n.n. Si at an edge between an hexagon and a pentagon, **3** and **4**: 2nd n.n. Si on a hexagon, resp. on a pentagon, **5**, **6** and **7**: 3rd n.n. Si, **8**: 4th n.n. Si and **9**: Si on opposite sides of the cage. The energy scale is given relatively to the energy of isomer **5**.

the two Si atoms are arranged just as in the experimentally determined structure of disilabenzene, in which two of the C atoms of the ring are replaced by two Si atoms [19].

It is interesting to notice that in the case of the boron-doped fullerenes  $C_{58}B_2$ , the two B atoms are predicted to lie as far as possible in the fullerene network [20] as indicated experimentally [1]. In contrast, recent photofragmentation experiments of  $C_{58}Si_2$  indicate that its initial fragmentation channel is the loss of  $Si_2$  [10]. This important observation suggests that the two Si atoms are not too far apart in the fullerene network and is consistent with our calculations.

## 4.2 Electronic structures of $C_{59}Si$ and $C_{58}Si_2$

The electronic structure of  $C_{59}Si$  and  $C_{58}Si_2$  are examined on the basis of a Kohn-Sham (KS) energy level analysis. Only the lowest energy  $C_{58}Si_2$  isomer is considered in this analysis. Since the icosahedral symmetry of  $C_{60}$  is broken in the doped fullerenes, the energy levels of  $C_{60}$  split. The Kohn-Sham energy levels of  $C_{59}Si$  and  $C_{58}Si_2$  derived from the 5-fold degenerate highest occupied energy levels (HOMO) and from the 3-fold degenerate lowest unoccupied energy levels (LUMO) of  $C_{60}$  are shown in Fig. 4.

Since silicon is isoelectronic to carbon (in terms of number of valence electrons) in-cage doping with silicon does

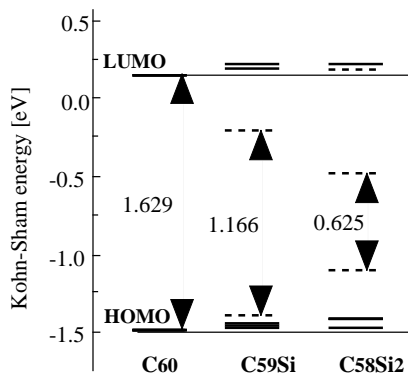


**Fig. 4.** Kohn-Sham energy levels of  $C_{60}$ ,  $C_{59}Si$  and  $C_{58}Si_2$  around the HOMO-LUMO energy gap. The dashed line represent strongly localized orbitals on the silicon atoms. The HOMO-LUMO gap is indicated for each molecule.

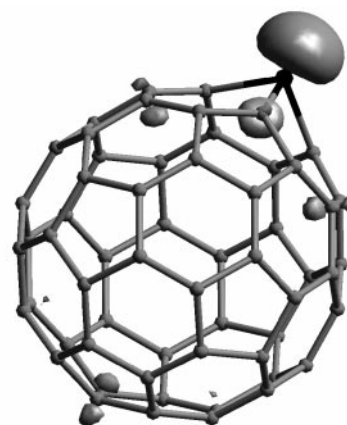


**Fig. 5.** Isodensity surface of the HOMO of  $C_{59}Si$  ( $0.004 \text{ e}/(\text{a.u.})^3$ ), showing that most of its probability density is localized on the Si atom shown by a black ball.

not change the total occupancy of the energy levels derived from those of  $C_{60}$ . This can be contrasted to boron- and nitrogen- in-cage doping of  $C_{60}$  where holes (boron) and electrons (nitrogen) are doped in the energy levels of  $C_{60}$  [3, 4, 20]. However due to the splitting of the energy levels in  $C_{59}Si$  and  $C_{58}Si_2$ , the HOMO-LUMO energy gap are reduced compared to the energy gap of  $C_{60}$ . The KS orbitals corresponding to the HOMO and LUMO of  $C_{59}Si$  are mainly localized on the Si atom, as shown in Fig. 5 in the case of the HOMO.

The same is true for  $C_{58}Si_2$  for which additionally the LUMO+1 and to a lesser extend the HOMO-1 show a localized probability density on the Si atoms. The energy separation between the pure carbon-like orbitals closest to these Si-like orbitals is close to the HOMO-LUMO energy gap of  $C_{60}$ . A substantial electronic charge transfer from the Si atom to the neighboring carbon atoms is observed (as for example from a Mulliken population analysis). This indicates that the bonds between Si and C are polar bonds. This is consistent with the smaller electronegativity of Si compared to that of C. Therefore in-cage doping with silicon introduces chemically distinct and reactive sites in the fullerene network while perturbing only moderately the electronic properties of the pure fullerene. This feature might be exploited in building self-assembled materials based on silicon-doped fullerenes.

I.M.L. B thanks the European Commission for funding under the "Training and Mobility of Researchers" program under grant No. ERB4001GT961173. The calculations were per-

formed on the CRAY-T3E-900/256 and T3E-600/512 computers in the Forschungszentrum Jülich with grants of CPU time from the German Supercomputer Center (HLRZ).

## References

1. T. Guo, C. Jin, R.E. Smalley: *J. Phys. Chem.* **95**, 4948 (1991)
2. T. Pradeep *et al.*: *J. Phys. Chem.* **95**, 10564 (1991)
3. W. Andreoni *et al.*: *Chem. Phys. Lett.* **190**, 159 (1992)
4. N. Kurita *et al.*: *Chem. Phys. Lett.* **198**, 95 (1992)
5. J.C. Hummelen *et al.*: *Science* **269**, 1554 (1995)
6. K. Prassides *et al.*: *Science* **271**, 1833 (1996)
7. T. Kimura *et al.*: *Chem. Phys. Lett.* **256**, 269 (1996)
8. J.L. Fye, M.F. Jarrold: *J. Phys. Chem. A* **101**, 1836 (1997)
9. M. Pellarin *et al.*: *Chem. Phys. Lett.* **277**, 96 (1997)
10. C. Ray *et al.*: *Phys. Rev. Lett.* **80**, 5365 (1998)
11. D.E. Clemmer *et al.*: *Nature* **372**, 248 (1994)
12. W. Branz *et al.*: *J. Chem. Phys.* **109**, 3425 (1998)
13. F. Tast *et al.*: *Phys. Rev. Lett.* **77**, 3529 (1996)
14. U. Zimmermann *et al.*: *Z. Phys. D* **31**, 85 (1994)
15. F. Tast *et al.*: *Z. Phys. D* **40**, 351 (1997)
16. R. Car, M. Parrinello: *Phys. Rev. Lett.* **55**, 2471 (1985)
17. N. Trouiller, J.L. Martins: *Phys. Rev. B* **43**, 1993 (1991)
18. K. Hedberg *et al.*: *Science* **254**, 410 (1991)
19. More precisely, in hexamethyl-1,4-disilabenzene, J.D. Rich, R. West: *J. Am. Chem. Soc.* **104**, 6884 (1982)
20. N. Kurita *et al.*: *Phys. Rev. B* **48**, 4850 (1993)